Electronic Supplementary Material (ESI) for Journal of Materials Chemistry C.

Supplementary Information

Template based Sintering of WO_3 Nanoparticles into Porous Tungsten Oxide Nanofibers for Acetone Sensing Applications

Muhammad Imran,[a] Syed Rashid,[b] Ylias Sabri,[b] Nunzio Motta,[a] Tuquabo Tesfamichael,[a] Prashant Sonar,[a] and Mahnaz Shafiei*[a, c]

[a]Institute for Future Environments and School of Chemistry, Physics, and Mechanical Engineering, Queensland University of Technology (QUT), Brisbane, QLD 4001, Australia

[b]School of Science, RMIT University, Melbourne, VIC 3000, Australia

[c]Faculty of Science, Engineering and Technology, Swinburne University of Technology, Hawthorn, VIC 3122, Australia

*Corresponding author email: mshafiei@swin.edu.au

Table S1. Effect of electrospinning parameters on mean fiber diameter of PVP/WO_3 composite NFs.

Sample	Voltage (KV)	Tip to collector distance (cm)	Feed rate (ml/hr.)	Mean fiber diameter (nm)
W1	9	12	1.2	1870
W2	10	12	1.2	1590
W3	11	12	1.2	1450
W4	12	12	1.2	1390
W5	13	12	1.2	1200
W6	14	12	1.2	1150
W7	15	12	1.2	1047
W8	9	16	1.2	1580
W9	10	16	1.2	1440
W10	11	16	1.2	1340
W11	12	16	1.2	1290
W12	13	16	1.2	1210
W13	14	16	1.2	1170
W14	15	16	1.2	1100
W15	9	16	0.6	1340
W16	10	16	0.6	1190
W17	11	16	0.6	1180
W18	12	16	0.6	1050
W19	13	16	0.6	1040
W20	14	16	0.6	820
W21	15	16	0.6	860

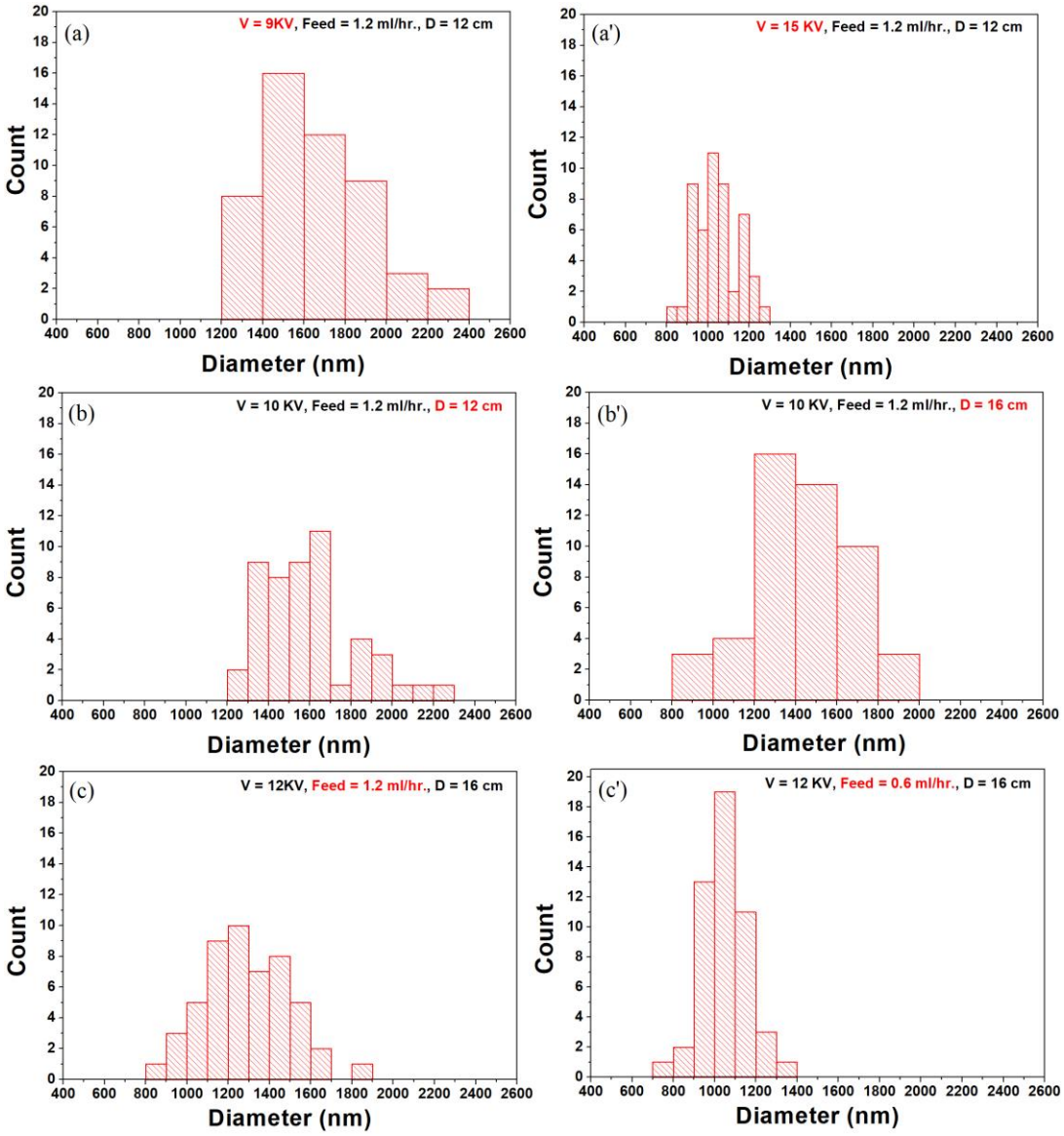

Figure S1. Fiber diameter distribution of PVP/WO_3 fibers electrospun at (a, a') 9 and 15 KV; (b, b') 12 and 16 cm; and (c, c') 1.2 ml/hr and 0.6 ml/hr, respectively.

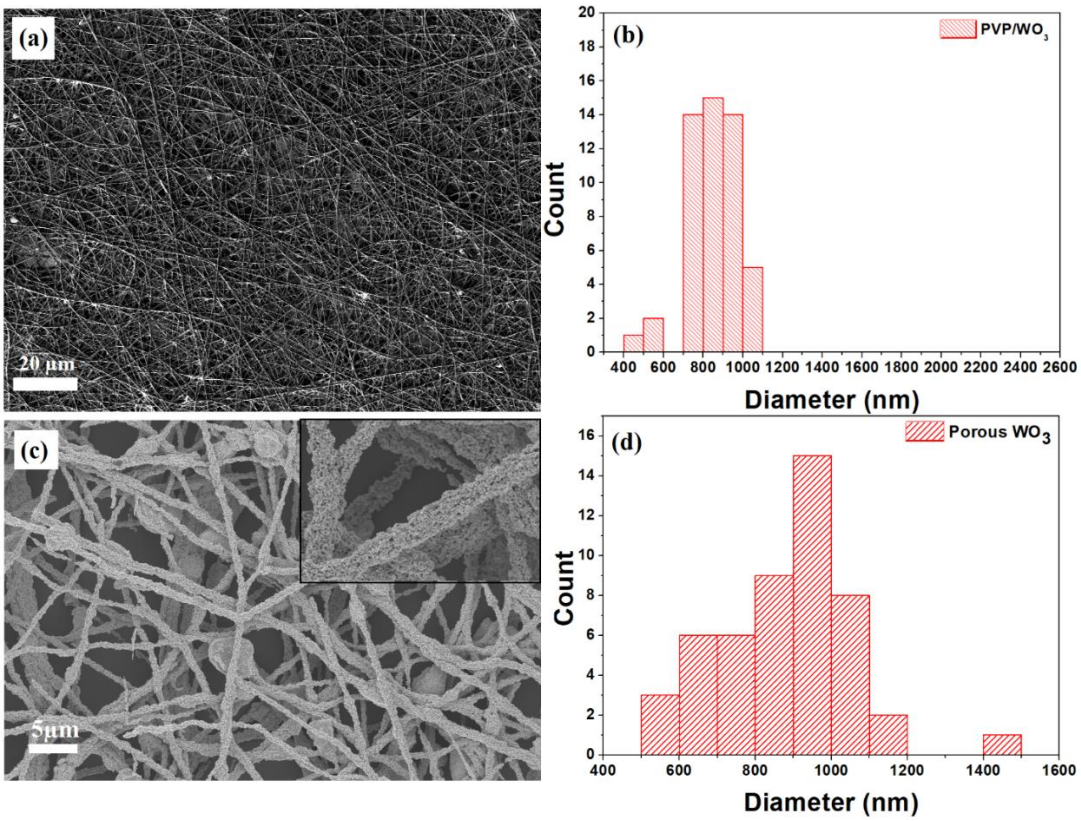

Figure S2. (a) SEM image, and (b) fiber diameter distribution of PVP/WO_3 composite NFs electrospun at 9 KV, with feed rate of 0.3 ml/hr and tip to collector distance of 16 cm. (c) SEM image (inset shows high resolution SEM image) and (d) fiber diameter distribution of porous WO_3 NFs after annealing.

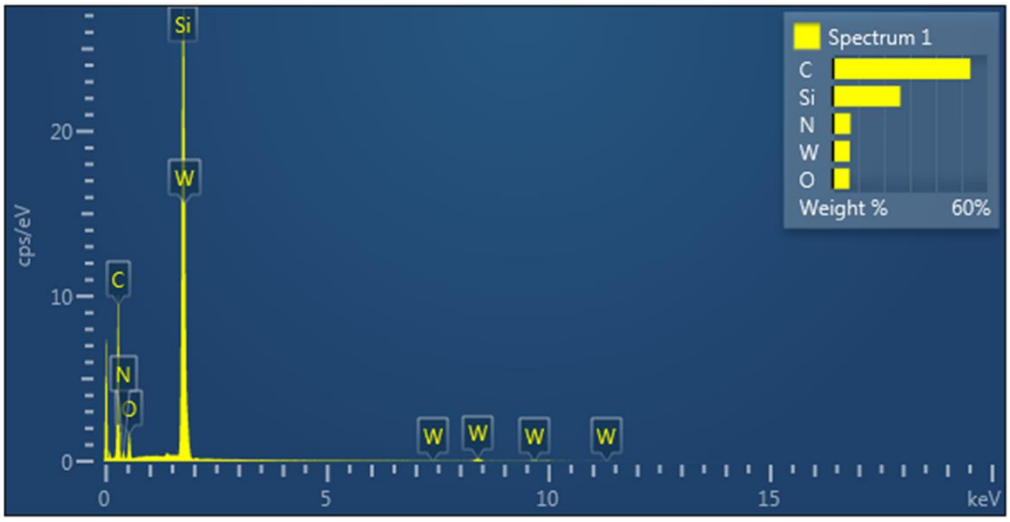

Figure S3: EDX analysis of PVP/WO_3 composite NFs.

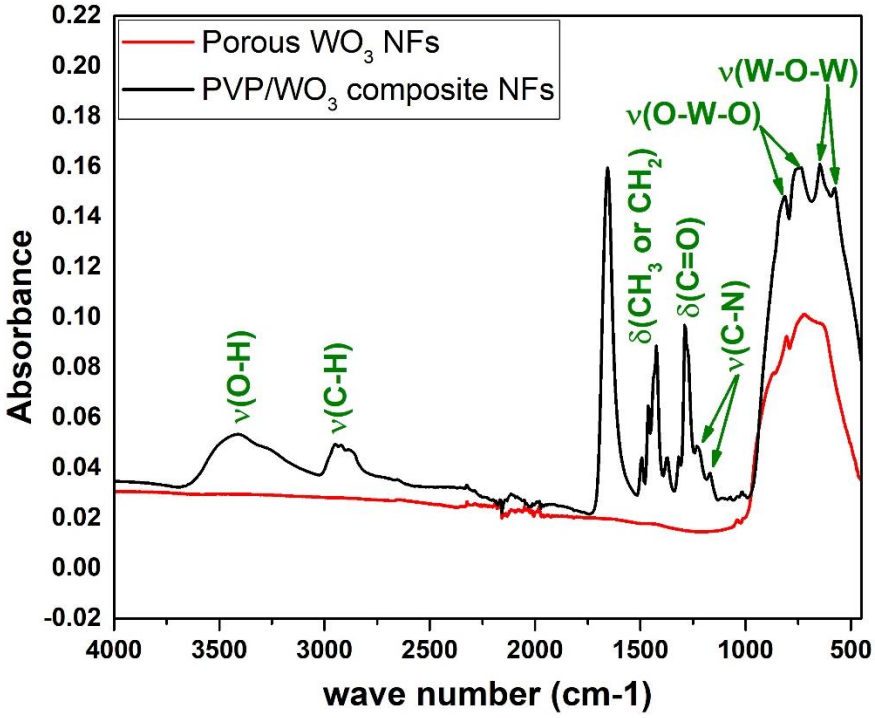

Figure S4. FTIR analysis of PVP/WO_3 composite NFs and porous WO_3 NFs.

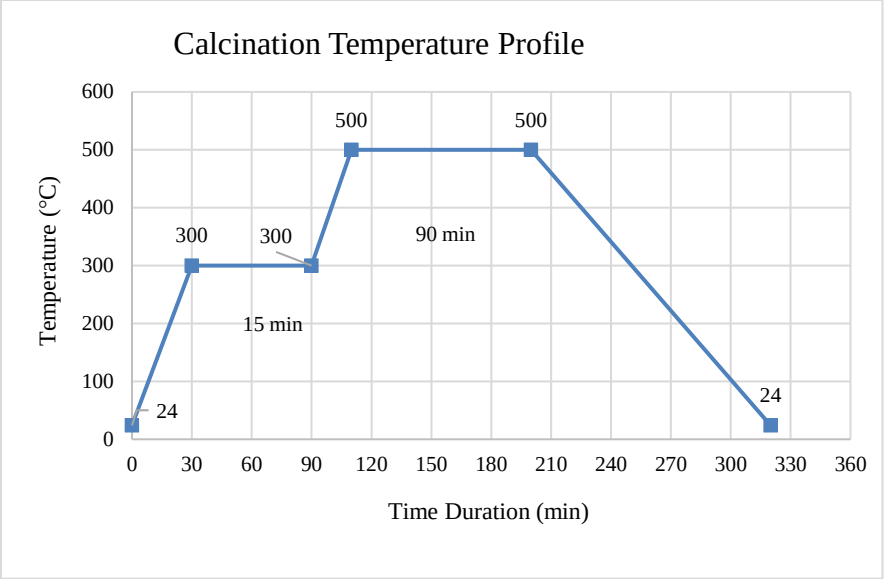

Figure S5. Temperature profile of annealing process.

Table S2. Annealing duration and temperature profile.

Sample code	Ramp rate	Temp1	Stay time1	Temp 2	Stay time 2
Sample 1	10 °C/min	-	-	500 °C	90 min
Sample 2	10 °C/min	300 °C	60	500 °C	90 min
Sample 3	10 °C/min	300 °C	30	500 °C	90 min
Sample 4	10 °C/min	300 °C	15	500 °C	90 min
Sample 5	10 °C/min	300 °C	15	550 °C	90 min
Sample 6	10 °C/min	300 °C	30	600°C	90 min
Sample 7	5 °C/min	300 °C	15	500 °C	90 min
Sample 8	2 °C/min	300 °C	15	500 °C	90 min

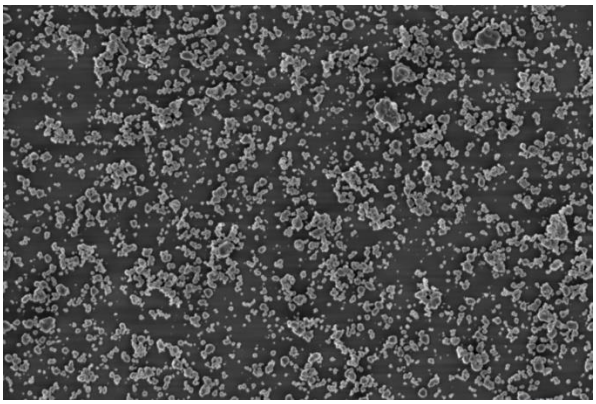

Sample 1

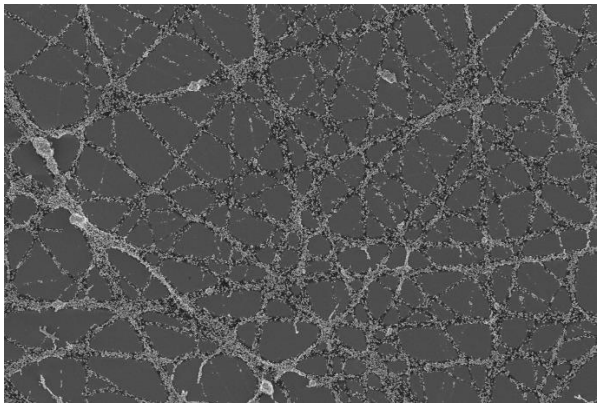

Sample 2

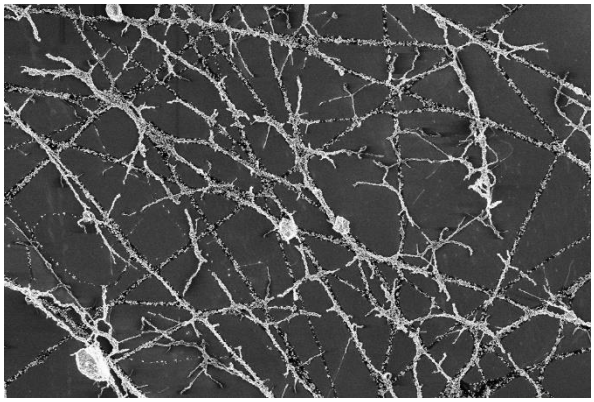

Sample 3

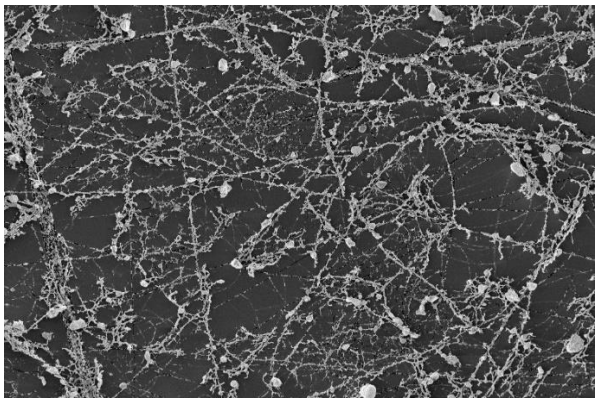

Sample 4

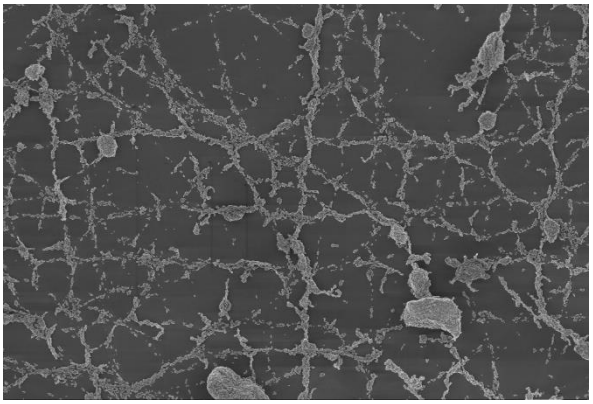

Sample 5

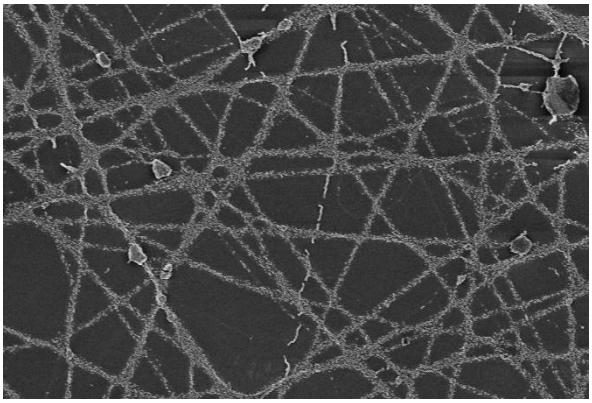

Sample 6

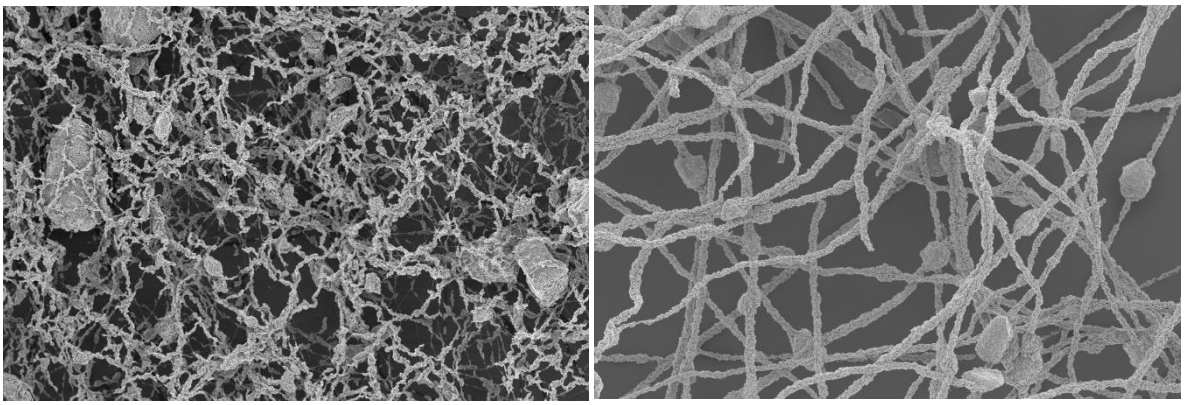

Sample 7 Sample 8

Figure S6. SEM images of calcined WO_3 nanofibers at different temperatures and stay time.

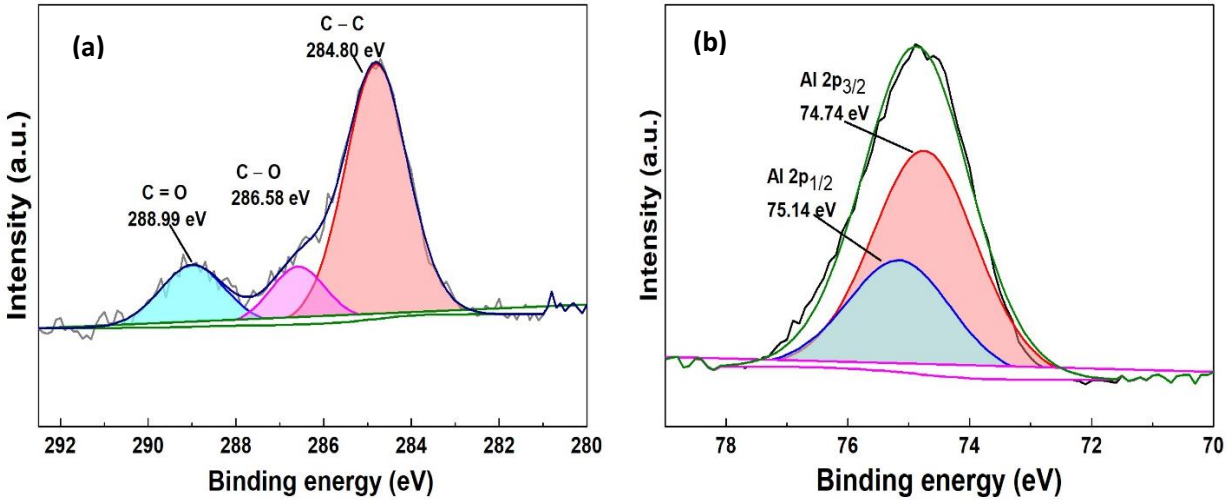

Figure S7: XPS high resolution spectra of C 1s and substrate (Al foil).

Table S3. Summarized sensing behavior of porous WO_3 NFs with biased voltage of 3 V at different operating temperatures.

Temperature	Dark	Light
30°C	No Response	Cannot differentiate the concentration
50°C	No Response	Cannot differentiate the concentration
150°C	No Response	Cannot differentiate the concentration
250°C	Can not differentiate the concentration	Cannot differentiate the concentration
350°C	Good response	Good response but sensitivity less than the dark

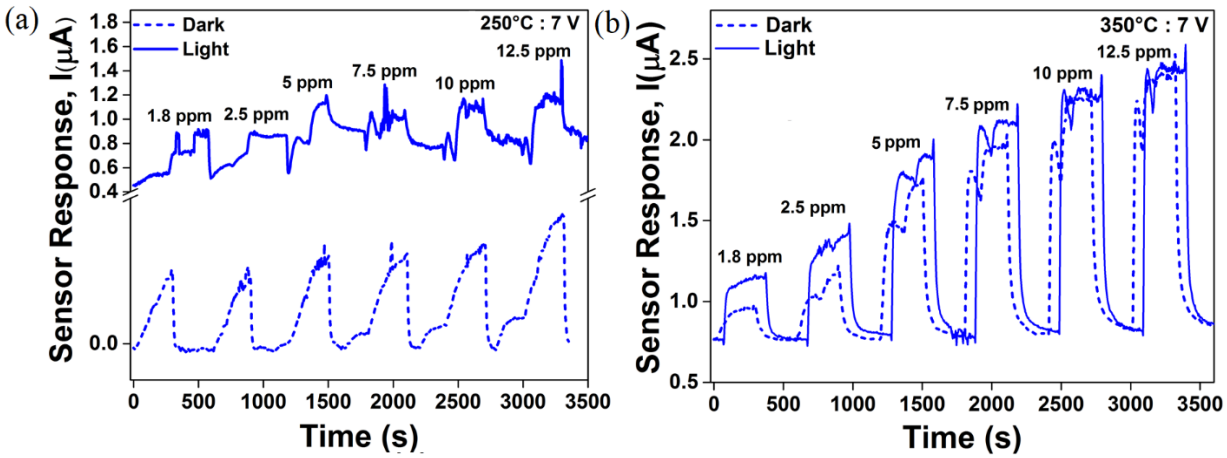

Figure S8. Dynamic response of porous WO_3 NFs at (a) 250 ℃; and (b) 350 ℃ with a bias voltage of 7 V toward acetone with different concentrations without and with UV irradiation (Dark and Light).

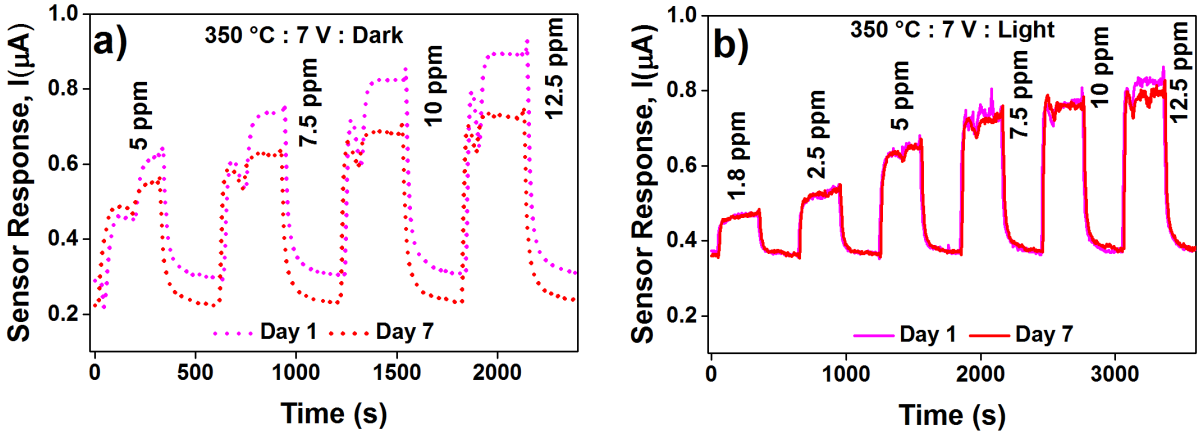

Figure S9. Stability of the sensor after 7 days.

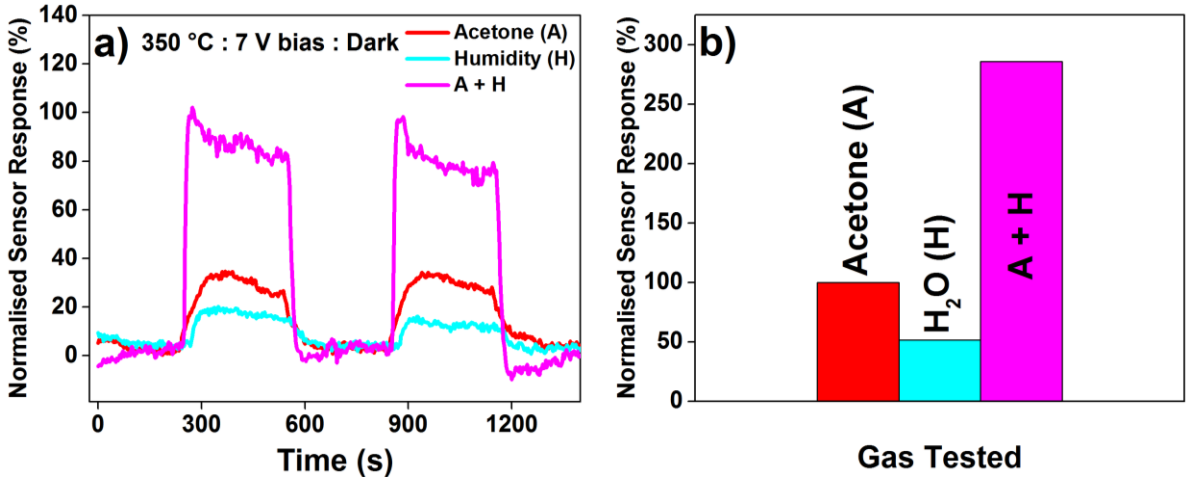

Figure S10. Selectivity of the porous WO_3 NFs in H_2O as interfering gas in dark toward 12.5 ppm acetone at 350 ℃.